LAWRENCE
LIVERMORE
NATIONAL
LABORATORY

UCRL-PROC-212821

Passivity of Alloy 22 in Chloride and Fluoride Containing Solutions

R. M. Carranza, M. A. Rodríguez, R. B. Rebak

June 10, 2005

16th International Corrosion Congress
Beijing, China
September 19, 2005 through September 24, 2005

To be presented at the 16th International Corrosion Congress (ICC), Beijing (China), 19-24 September 2005

PASSIVITY OF ALLOY 22 IN CHLORIDE AND FLUORIDE CONTAINING SOLUTIONS

***Ricardo M. Carranza[1], Martín A. Rodríguez[1], Raúl B. Rebak[2]**
[1]Comisión Nacional de Energía Atómica, Buenos Aires, Argentina
[2]Lawrence Livermore National Laboratory, Livermore, CA, USA

Abstract

The aim of the present work was to study the passive behavior of Alloy 22 in chloride and fluoride containing solutions varying the heat treatment of the alloy, the halide concentration and the pH of the solution at 90°C. General corrosion behavior was studied using electrochemical techniques, which included open circuit potential monitoring over time, potentiodynamic polarization and electrochemical impedance spectroscopy (EIS) measurements carried out at open circuit and at passive potentials. Corrosion rates obtained by EIS measurements after 24 h immersion were below 0.5 μm/year. The corrosion rates were practically independent of the solution pH, short term corrosion potential (E_{corr}), alloy heat treatment and halide ion nature and concentration. Polarization resistance (R_P) values increased with open circuit potential and the polarization time at constant potential in 1M NaCl, pH 6, 90ºC. This was attributed to an increase in the oxide film thickness and oxide film aging. Capacitance measurements indicated that passive oxide on Alloy 22 presented a double n-type/p-type semiconductor behavior in the passive potential range.

Keywords: N06022, passivity, corrosion rate, chloride, fluoride, oxide growth

1. Introduction

The engineered barriers for the permanent disposal of high-level nuclear waste in Yucca Mountain are designed to maintain isolation of the waste for thousand of years. These barriers include a double wall metallic container and a detached drip shield.[1] Alloy 22 (N06022) was selected for the outer shell of the container[1]. The primary purpose of the outer shell is to provide protection against corrosion. If water is present in the repository site, Alloy 22 may undergo different corrosion processes, namely, general or uniform corrosion, stress corrosion cracking, and localized corrosion.[2] The environment at Yucca Mountain is basically dry. It is possible for aqueous solutions to contact the container surface. These solutions may form via dripping from the drift wall or by deliquescence of dust that may accumulate on the container surface. Chloride is one of the most detrimental species since it may promote crevice corrosion in Alloy 22 under specific conditions. Different concentrations of fluorides and chlorides can be naturally found in ground waters. While the effects of chlorides on the passive state and localized corrosion have been extensively studied for austenitic alloys which form chromium oxide films, the effects of fluorides have not been fully characterized.[3,4,5,6] The maximum allowed temperature by design specifications is 350ºC.[1] Tetrahedral close packed (TCP) phases precipitate in Alloy 22 only at temperatures of 593ºC or higher.[7,8,9] These phases could have a detrimental effect upon corrosion resistance and cause loss of mechanical ductility. A long

range ordering reaction (LRO) can occur at lower temperatures and produce an ordered $Ni_2(Cr,Mo)$ phase.[7] This ordering reaction is thought to cause little or no effect on corrosion and causes only a slight loss in ductility.

The aim of this study was to investigate the effects of pH and thermal aging on the susceptibility of Alloy 22 to general corrosion in chloride, fluoride, and mixtures of chloride-fluoride solutions at 90ºC. The results presented in this study correspond to solutions containing a much larger amount of chloride and fluoride than in the ground water at Yucca Mountain, which are approximately 7 mg/L and 2 mg/L, respectively. 1 M fluoride represents 19,000 mg/L and 1 M chloride represents 35,000 mg/L; these values are 5,000 to 10,000 times the concentration of halide in the ground water.

2. Experimental Procedure

Specimens of Alloy 22 were prepared from wrought mill annealed plate stock (MA specimens). The chemical composition of the alloy in weight percent was 59.20% Ni, 20.62% Cr, 13.91% Mo, 2.68% W, 2.80% Fe, 0.01% Co, 0.14% Mn, 0.002% C, and 0.0001% S. Some specimens were aged for 10 h at 760ºC (TCP specimens) and 1,000 h at 538ºC (LRO specimens). Aging was performed in air and the specimens were quenched in water after the heat treatment. Parallelepiped specimens measuring 12 mm x 12 mm x 15 mm were mounted with a PTFE compression gasket (ASTM G 5)[10]. The exposed area of the specimen was 10.5 cm^2. The specimens had a finished grinding of abrasive paper number 600 and were degreased in acetone and washed in distilled water 1 hour prior to testing.

Electrochemical measurements were conducted in a three-electrode, borosilicate glass cell. A water-cooled condenser combined with a water trap was used to avoid evaporation and the ingress of air. Solution temperature was controlled by immersing the cell in a thermostatisized water bath. The cell was equipped with both an air cooled Luggin and a saturated calomel reference electrode (SCE). A large area platinum wire mesh was used as a counter electrode. The electrochemical tests were carried out in three different solutions: 1M NaCl, ~1 M NaF (concentration corresponding to a saturated solution at room temperature) and 0.5 M NaCl + 0.5 M NaF at pH values of 2, 6 and 9. Small amounts of HF, HCl, or NaOH were added in order to adjust solution pH. The test temperature was 90ºC. Only the solutions for the potentiodynamic polarization curves were deaerated with nitrogen, all the others were naturally aerated, that is, air was not bubbled through the solution. Electrochemical Impedance Spectroscopy (EIS) measurements were carried out at the corrosion potential and at passivity potentials in aerated solutions. A 10 mV amplitude sinusoidal potential signal was superimposed to the corrosion potential. The frequency scan was started at 10 kHz and ended at 1 mHz. In other experiments the capacitance of the interface (C) was calculated from the imaginary part of the impedance (Z") at a frequency of 1 kHz. These specimens were previously polarized at -0.800 Vsce for 5 minutes, and then the passive oxide was grown at a fixed potential of 0.100 Vsce for 2 hours. The applied potential was changed, stepwise, in the less noble direction and the impedance was measured at each potential.

3. Results and Discussion

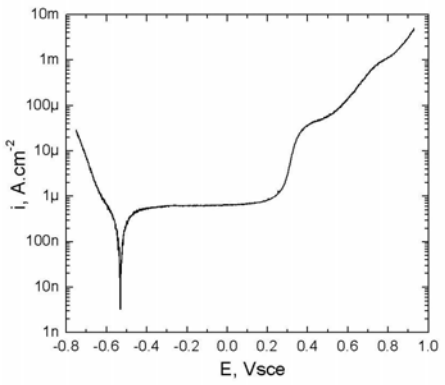

Fig. 1: Potentiodynamic polarization curve of Alloy 22 (MA) in NaCl 1M pH 6 at 90ºC - N_2 bubbling - 0.167mV/s.

Figure 1 shows a typical polarization curve for MA Alloy 22 in 1M NaCl at pH 6. This curve, as well as those for the other solutions tested here, presented a relatively wide passive zone with very low passive currents approximately independent of applied potential. After the passive domain, the anodic current increased with increasing potential due to a transpassivation reaction usually associated to chromium depletion from the passive film. Passivity breakdown potential was reported to be pH dependent but passive current densities are slightly dependent on pH for pH values between 2 and 9.[11,12]

Electrochemical impedance spectroscopy measurements were performed, on MA Alloy 22 in 1M NaCl at pH 6, at different applied potentials between the corrosion potential and the transpassivity potential. Different impedance diagrams were obtained depending on the applied potential. At the less anodic potentials (near the corrosion potential), two or three time constants were visualized, while in the full passive range at the more anodic applied potentials only one time constant was visualized in the impedance diagrams (Fig. 2).

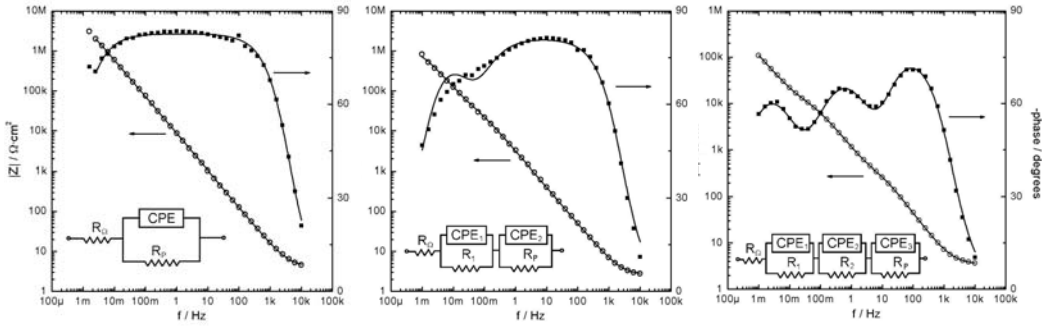

Fig. 2: Bode diagrams corresponding to EIS measurements of Alloy 22 (MA) in NaCl 1M pH 6 at 90ºC at fixed potentials of 0.100 Vsce, -0.400 Vsce and -0.500 Vsce. Points: exp. data - Lines: fitting of equivalent circuits indicated in graphics.

In order to model the impedance results with electrical analogs, simplified R//CPE series equivalent circuits were used as depicted in Figure 2. A simplified R//C series equivalent circuit was used by other workers [13] for Alloy 22 in NaCl brines at elevated temperature in order to model impedance diagrams in the full passive range attributing three time constants: one for the metal/film interface, a second one to the barrier layer film and the last one to the film/solution interface. In the present work, the main interest was to trace the low frequency resistance (R_p), so these three time constants of the full passive range are represented here by only one R//CPE and the low frequency resistance obtained corresponded to the total resistance calculated in that work[13]. The high frequency time constants, at the more cathodic potentials (not in the full passive range) were interpreted as associated to the cathodic reactions and to the oxidation of Ni at potentials closer to the reversible potential where the oxide layer is supposed to be thinner.

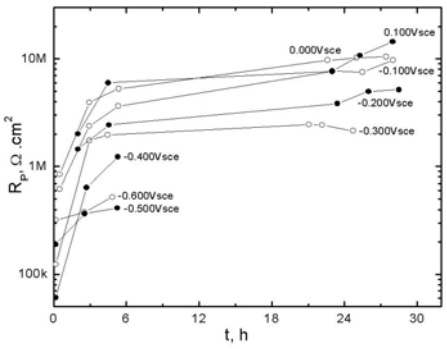

Fig. 3: Polarization resistance (Rp) as a function of polarization time of Alloy 22 (MA) in NaCl 1M pH 6 at 90ºC for different passivity potentials.

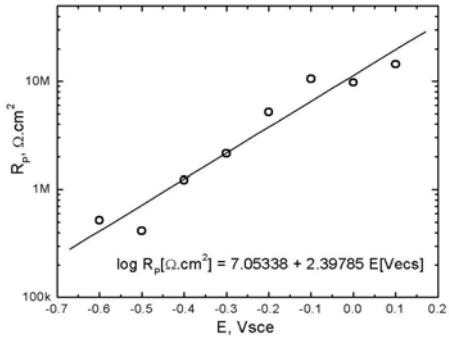

Fig. 4: Polarization resistance (Rp) at 24 h. of polarization as a function of potential (E) of Alloy 22 (MA) in NaCl 1M pH 6 at 90ºC. Points: exp. data - Line: log. Fitting.

Figure 3 shows the variation of Rp values, obtained by fitting of the equivalent circuits to the experimental impedance diagrams, as a function of time of immersion for different applied potentials. A fast increase of Rp was observed during the first hours of immersion followed by a slow increase later on. The variation of the Rp values obtained after 24h immersion at each applied potential is shown in Figure 4. A linear behavior of log(Rp) with potential was observed. A linear behavior is expected for the film thickness with potential in all valve metals[14], as was indirectly obtained on Alloy 22 in concentrated brines [15], assuming that geometric capacitance of the oxide layer can be estimated from the imaginary component of the interfacial impedance at very high frequencies. Thus, the low frequency resistance Rp was interpreted in these measurements as being mainly related to the oxide barrier layer thickness. However, it is commonly understood that passive films in iron-chromium and nickel-chromium alloys behave as semiconductors [16,17,18]. Figure 5 shows the results of the capacitance measurements on the passive films formed on Alloy 22, plotted as C^{-2} vs. potential,(E). Two linear regions revealing Mott-Schottky behavior are apparent and they can be related to the development of depletion layers promoted by band bending.

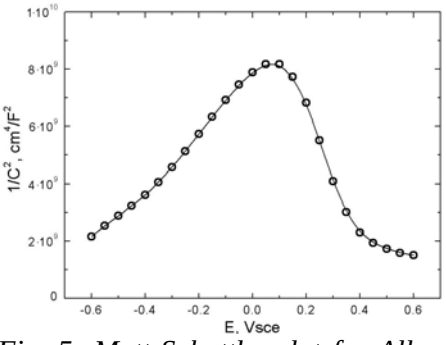

Fig. 5: Mott-Schottky plot for Alloy 22 (MA) in NaCl 1M pH 6 at 90ºC.

When the film was polarized at the less noble potentials it behaved as a n-type semiconductor (positive slope) and when the polarization was in the domain of the more noble potentials its behavior was that of a p-type semiconductor (negative slope). This result is in line with that obtained by Macdonald *et al* in saturated NaCl solutions [15]. The authors attribute the n-type semiconducting behavior to the dominant defects in the film being chromium interstitials and/or oxygen vacancies.

They proposed that the most likely explanation for the change in electronic character is the generation of cation vacancies (electronic acceptors and hence p-type dopants) at the film|solution interface through the oxidative ejection of cations from the film. This explanation seems fairly reasonable, but in the present work, the potential attributed to the change in electronic character of the passive film (around 0.0 Vsce Fig. 5) was found to be 300 mV below the initiation of transpassive dissolution (around 0.3 Vsce Fig. 1).

In another set of experiments, using 1 M NaCl, 1 M NaF and 0.5 M NaCl + 0.5 M NaF in aerated conditions, the freely corroding potential was monitored and was found to be higher than that displayed in deaerated conditions and increased continually with time of exposure as can be shown in figure 6 for 1 M NaCl at pH 6. Electrochemical impedance spectroscopy measurements were performed at E_{corr} following its evolution with time. One or two time constant impedance diagrams were obtained depending on E_{corr} values, and simplified R//CPE series equivalent circuits were again used (Fig. 2) in order to model the impedance behavior. This time, the low frequency resistance (Rp) was used to calculate the corrosion rate assuming a linear relationship between Rp^{-1} and the corrosion rate (CR) as it is usually done [15,19]:

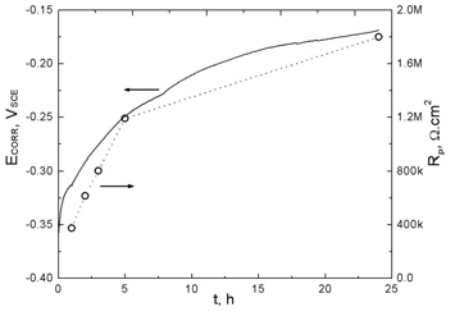

Fig. 6: Free corrosion potential (Ecorr) and polarization resistance (Rp) over immersion time for Alloy 22 (MA) in NaCl 1M pH 6 at 90ºC.

$$CR(mm/yr) = \frac{K\, i_{corr}\, EW}{\rho} \text{ with } i_{corr} = \frac{B}{R_p}$$

where i_{corr} is the corrosion current density in A/cm^2, EW is the equivalent weight (23.28, assuming congruent dissolution of the major alloying elements as Ni^{2+}, Cr^{3+}, Mo^{3+}, Fe^{3+}, and W^{4+}), K is the faradaic conversion factor (3,270 mm g A^{-1} cm^{-1} yr^{-1}), ρ is the density (8.69 g/cm^3)(ASTM G102[10]), and B is the Stern and Geary constant[20]. The latter can be calculated using Tafel slopes attributed to the anodic and the cathodic processes occurring at the corrosion potential. Macdonald *et al.* [15] found a constant passivation current density independent of the potential for Alloy 22 in NaCl brine at 80ºC, this indicate that the Stern and Geary constant would be dominated by the cathodic Tafel slope ($B = \beta_c / 2.303$), but in a previous paper[13] they measured the anodic (different from ∞) and cathodic Tafel slopes using potentiodynamic polarization curves, obtaining B values between 24 and 46 mV for solution pH values varying from 1.0 to 8.1. In the present work the Stern and Geary constant used in calculating the corrosion rate was assumed to be 26 mV (the all purpose middle value, expected for both theoretically calculated and experimentally observed values, as proposed by Mansfeld [21]) independently of the solution composition and pH, and it is not intended to represent the real value of the B constant but a sort of mean value useful for the sake of comparison. Figure 7 shows the CR values obtained for all the solutions and pH tested in this work as a function of E_{corr}. The reported CR values included measurements up to a maximum of 24 h of immersion at 90ºC in aerated conditions. For all the systems tested it can be said that CR decreased with E_{corr} (or time) independently of the solution composition, pH and alloy microstructure. The calculated CR values varied from near 10 $\mu m.yr^{-1}$, for the lowest initial E_{corr}, to as low as 0.03 $\mu m.yr^{-1}$ for impedances measurements performed at E_{corr} values attained

after 24h of immersion. If the passive current density (i.e. the corrosion rate) is independent of potential as it appears to be from potentiodynamic polarization curves performed at low potential scan rates [11,12] and as was measured in NaCl brine at 80ºC [15], and also as predicted from the Point Defect Model [22], then the decline of the corrosion rate, as time increases, must be attributed to film thickening during the first hours of immersion. The observed fast increase of Rp with time at different applied anodic potentials supports this hypothesis (Fig. 3). But after a certain period of time, film thickening would stop (due to a dynamic equilibrium between film growth and dissolution [15]) and all later decrease in corrosion rate and/or passive current density would be due to film aging by annihilation of defect sites as proposed elsewhere [23]. While short term general corrosion rates (i.e., those measured over periods of hours to weeks, generally measured using electrochemical methods) range from 1.0 to 0.1 μm/year [11,12,13], long term rates (measured over >5-year periods using weight loss techniques [24]) slow down to a few nanometers per year, thus sustaining the idea of film improvement with time due to annihilation of defects.

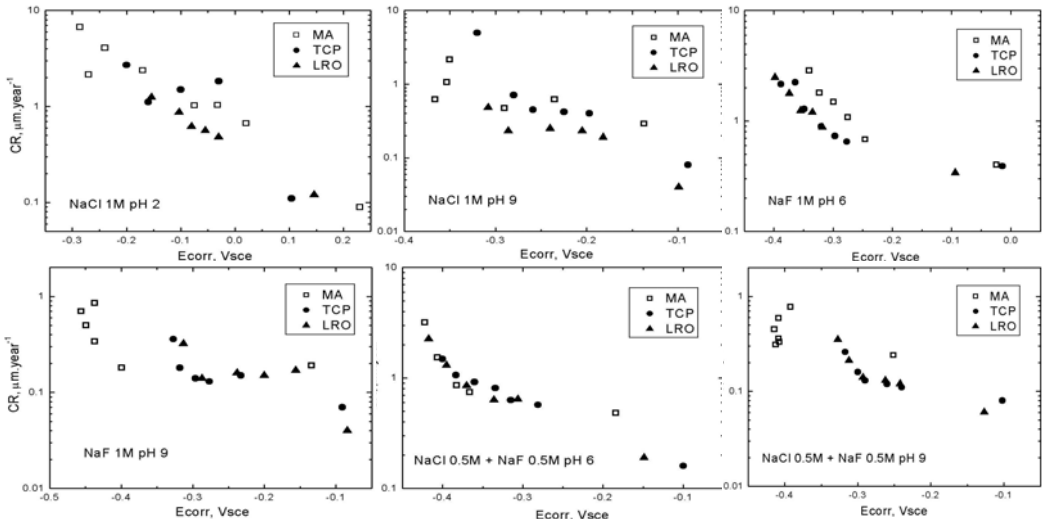

Fig. 7: Corrosion Rate (CR) of Alloy 22 (MA, TCP and LRO) in different solutions at 90ºC as a function of corrosion potential (Ecorr).

From figure 7 it can also be observed that the corrosion rates were slightly affected by solution pH and E_{corr} and to a lesser extent by alloy heat treatment and by the identity of the halide ion and its concentration.

5. Conclusions

1. Low frequency resistances obtained from EIS measurements at anodic potentials applied in the passive range of Alloy 22 in chloride environments were associated to the barrier layer thickness. The change in its semiconductor character, from n-type to p-type, could not be associated in this system to the onset of transpassivity.

2. Low frequency resistances obtained from EIS measurements at corrosion potentials for Alloy 22 in concentrated chloride, fluoride and mixed fluoride/chloride solutions at 90ºC were used to calculate mean corrosion rate values that rendered a time decreasing corrosion rate associated to film growth at the initial periods of immersion and to film aging by annihilation of defects sites later on.

3. Passive films formed at the freely corroding potential on Alloy 22 after 24 h of immersion, rendered enough protection to the base alloy to give corrosion rates lower than 0.5 μm yr^{-1}, independently of the solution composition, the pH and the microstructure of the alloy.

Acknowledgments

This work was partially performed under the auspices of the U. S. Department of Energy by the University of California Lawrence Livermore National Laboratory under contract N° W-7405-Eng-48. This work is supported by the Yucca Mountain Project, which is part of the Office of Civilian Radioactive Waste Management (OCRWM)

6. References

[1] G. M Gordon, Corrosion, 58, 811 (2002)
[2] R.B. Rebak and J. C. Estill, Materials Research Society, Warrendale PA, 2003, Volume 757, pp. 713-721.
[3] G.H. Koch, MTI Publication 41, Mat. Tech. Inst. of the Chemical Process Industries Inc., Columbus, Ohio, Published by NACE International, 1995.
[4] G.H. Koch, N.G. Thompson, J.L Means, EPRI Report CS-4374, Palo Alto, CA, 1986.
[5] G.H. Koch, G.W. Kistler, W. Mirich, EPRI Report CS-5476, Palo Alto, CA, 1987.
[6] N.S. Meck, P. Crook, R.B. Rebak in Corrosion Science, A Retrospective and Current Status in Honor of Robert P. Frankenthal, PV 2002-13, The Electrochemical Society, Pennington, NJ, 2002, pp. 355-368.
[7] M. Raghavan, B.J. Berkowitz, J.C. Scanlon, Met. Trans., 1982, 13A, pp. 979.
[8] H.M. Tawancy, J. Mater. Sci., 1996, 31, pp. 3929.
[9] F.G. Hodge, H.S. Ahluwalia, Proc. 12th Int. Corrosion Congress, Houston, TX, NACE International, 1993, 5B, pp. 4031.
[10] Annual Book of ASTM Standards, Volume 03.02, West Conshohocken, PA (2001).
[11] M. A. Rodríguez, R. M. Carranza, R. B. Rebak, *Metall. Trans. A*, 2005, **36/5**, 1179-1185.
[12] M. A. Rodríguez, R. M. Carranza, R. B. Rebak, paper 04700, Corrosion/04, NACE International, Houston, TX, 2004, pp. 1-13.
[13] N. Priyantha, P. Jayaweera, D. D. Macdonald, A. Sun, *J. Electroanal. Chem*., 2004, **572**, 409-419.
[14] L. Young, Anodic Oxide Films, Academia Press, New Cork, NY, 1961.

[15] D. D. Macdonald, A. Sun, N. Priyantha, P. Jayaweera, *J. Electroanal. Chem.*, 2004, **572**, 421-431.
[16] M. G. S. Ferreira, N. E. Hakiki, G. Goodlet, S. Faty, A. M. P. Simões, M. Da Cunha Belo, *Electrochim. Acta* 2001, **46**, 3767–3776.
[17] N. E. Hakiki, M. Da Cunha Belo, A. M. P. Simões, M. G. S. Ferreira, *J.Electrochem. Soc.* 1998, **145/11**, 3821–3828.
[18] M. Da Cunha Belo, N. E. Hakiki, M. G. S. Ferreira, *Electrochim. Acta* 1999, **44**, 2473–2481.
[19] D. D. Macdonald, M. C. H. McKubre, in Impedance Spectroscopy, Theory, Experiment, and applications, 2nd Ed., E. Barsoukov and J. R. Macdonald eds., John Wiley & Sons, New Jersey, 2005, 343.
[20] M. Stern, A. L. Geary, *J. Electrochem. Soc.*, 1957, **104**, 56.
[21] F. Mansfeld, in Adv. In Corrosion Science and Technology Vol. VI, M. G. Fontana and R. W. Staehle, eds., Plenum Press, New York, 1976, 163-262.
[22] D. D. Macdonald, *Pure Appl. Chem.*, 1999, **71**, 951-986.
[23] B. R. MacDougall, in Proc. Int. Works. on Long-Term Passive Behavior, A. A. Sagüés, C. A. W. Di Bella, eds., Virginia,VA, U. S. Nuc. Waste Tech. Rev. Board, 2001, 49-54.
[24] L. L. Wong, D. V. Fix, J. C. Estill, R. D. McCright, R. B. Rebak, Materials Research Society, Warrendale, PA, 2003, Vol. 757, 735-741.